

WD-A191 715

EFFECTS OF SECONDARY STRUCTURE ON THE STRESS AND
STABILITY OF SUBMARINE PRESSURE HULLS(U) DEFENCE

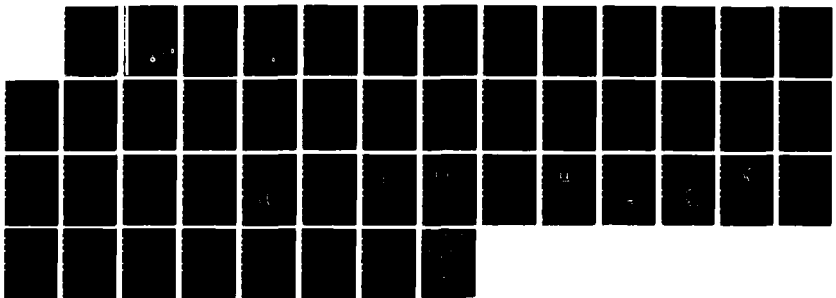
1/1

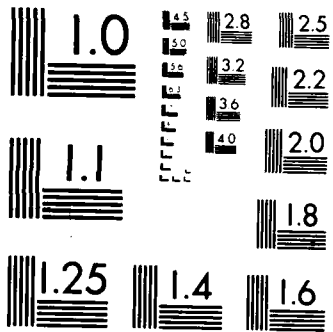
RESEARCH ESTABLISHMENT ATLANTIC DARTMOUTH (NOVA SCOTIA)

UNCLASSIFIED

N G PEGG NOV 87 DREA-87/102

F/G 13/10 1 NL





UNLIMITED DISTRIBUTION



National Defence
Research and
Development Branch

Défense Nationale
Bureau de Recherche
et Développement

DTIC FILE COPY

REPORT 87/102

November 1987

AD-A191 715

EFFECTS OF SECONDARY STRUCTURE
ON THE STRESS AND STABILITY
OF SUBMARINE PRESSURE HULLS

Neil G. Pegg

DTIC
SELECTED
JAN 26 1988
S E D
E

Defence
Research
Establishment
Atlantic



Centre de
Recherches pour la
Défense
Atlantique

Canada

88 1 20 047

DEFENCE RESEARCH ESTABLISHMENT ATLANTIC

9 GROVE STREET

P.O. BOX 1012
DARTMOUTH, N.S.
B2Y 3Z7

TELEPHONE
(902) 426-3100

CENTRE DE RECHERCHES POUR LA DÉFENSE ATLANTIQUE

9 GROVE STREET

C.P. 1012
DARTMOUTH, N.B.
B2Y 3Z7

UNLIMITED DISTRIBUTION



National Defence Défense Nationale
Research and Bureau de Recherche
Development Branch et Développement

EFFECTS OF SECONDARY STRUCTURE
ON THE STRESS AND STABILITY
OF SUBMARINE PRESSURE HULLS

Neil G. Pegg

November 1987

Approved by B.F. Peters A/Director/Technology Division

DISTRIBUTION APPROVED BY

CHIEF D.R.E.A.

REPORT 87/ 102

Defence
Research
Establishment
Atlantic



Centre de
Recherches pour la
Défense
Atlantique

Canada

Abstract

This report presents an investigation into the localized effects of secondary structure such as decks, tanks and cutouts, and other deviations from axisymmetry on the global failure load estimation of axisymmetric submarine pressure hulls. Three dimensional finite element analysis predictions of stress, elastic bifurcation buckling, and nonlinear collapse loads of a representative complete section of a conventional submarine are compared to those of axisymmetric analysis methods applied to the pressure hull alone. Four different methods of analyzing the basic axisymmetric pressure hull are also compared. Stress patterns, buckling mode shapes and failure loads of the fully developed structural models were found to differ significantly from those obtained assuming complete axisymmetry. The inclusion of decks and tanks increased the failure loads, whereas cutouts and dents in the pressure hull lowered the failure loads. In addition to analytical results, experimental strain measurements made on an Oberon class pressure hull are compared to finite element predictions. (Caro da)

Résumé

Le présent rapport expose une étude des effets localisés de structures secondaires, tels les ponts, réservoirs et découpes, et d'autres écarts de symétrie axiale sur les estimations de la rupture globale des coques de sous-marin à symétrie axiale. Des méthodes de prévision par analyse tridimensionnelle à éléments finis des contraintes, du flambage de bifurcation élastique et de charges d'écrasement non linéaire pour une section complète d'un sous-marin classique sont comparées aux méthodes d'analyse à symétrie axiale appliquées à la seule coque de pression. Sont également comparées quatre méthodes différentes d'analyse de la coque de pression de base à symétrie axiale. Il a été constaté que les modes de contraintes et de flambage ainsi que les charges de rupture données par les modèles structurels complets diffèrent significativement de ceux qu'on obtient en faisant l'hypothèse de la symétrie axiale totale. L'incorporation de ponts et de réservoirs fait augmenter les charges de rupture, tandis que l'inclusion de découpes et d'indentations dans la coque de pression les fait abaisser. Outre les résultats analytiques, des mesures de contraintes expérimentales faites sur des coques de pression de classe Oberon sont comparées aux prévisions des méthodes à éléments finis.

Accession For	
NTIS GRA&I	<input checked="" type="checkbox"/>
DTIC TAB	<input type="checkbox"/>
Unannounced	<input type="checkbox"/>
Justification	
By _____	
Distribution/ _____	
Availability Codes	
Dist	Avail and/or Special
A-1	



Contents

Abstract	ii
Table of Contents	iii
List of Tables	iv
List of Figures	iv
Notation	vi
1 Introduction	1
2 Criteria for Pressure Hull Strength	6
2.1 Stress in Ring Stiffened Cylinders	6
2.2 Buckling Stability of Ring Stiffened Cylinders	7
3 Analytical Solution Methods	9
3.1 Equation Based Solutions	9
3.2 Axisymmetric Analysis	9
3.2.1 Axisymmetric Finite Difference Analysis	10
3.2.2 Axisymmetric Finite Element Analysis	10
3.3 Three Dimensional Analysis	11
3.3.1 Linear Analysis	11
3.3.2 Nonlinear Analysis	12
3.3.3 Three Dimensional Finite Element Structural Models	12
4 Experimental Strain Measurements	19
5 Results and Discussion	20
5.1 Comparison of Methods for Axisymmetric Pressure Hull Analysis	20
5.2 Comparison of Three Dimensional Models with Secondary Structure	24
5.2.1 Stress Results	24
5.2.2 Overall Buckling Results	27
5.2.3 Interframe Buckling Results	31
5.2.4 Plastic Collapse Results	33
5.3 Strain Measurements	34
6 Conclusions	36

List of Tables

1	Comparison of Predictions for Axisymmetric Pressure Hull Alone	20
2	Comparison of Predictions for Secondary Structure on Pressure Hull	24
3	Comparison of Experimental and Theoretical Stress Values	34

List of Figures

1	Cross Section of Submarine Geometry	1
2	Interframe Elastic Bifurcation Buckling Mode Shape of A Ring Stiffened Cylinder	2
3	Overall Elastic Bifurcation Buckling Mode Shape of A Ring Stiffened Cylinder .	3
4	Deflection vs Load Relationship of Three Failure Mechanisms	3
5	Three Catagories of Analysis Methods	4
6	Critical Stress Points in A Ring Stiffened Cylinder	6
7	Frame Buckling Failure Mode	8
8	Axisymmetric Model of A Typical Submarine Pressure Hull	10
9	Axisymmetric Finite Element Model of the Pressure Hull Section	11
10	Stress Strain Material Curve Used in Nonlinear Analysis	12
11	MODEL 1 - A three dimensional half model of a length of axisymmetric pressure hull between bulkheads, with shell plating and six T-bar stiffeners.	13
12	MODEL 2 - Model 1 with a large dent modelled between two stiffeners on the side of the pressure hull. The dent is sinusoidal in shape with a maximum depth equal to the frame depth and a half period equal to the length between stiffeners.	14
13	MODEL 3 - Model 1 with the trim tank added which consisted of a deck on top and a vertical bulkhead on its side. The deck and bulkhead stiffeners were modelled by smearing them into equivalent plating.	15
14	MODEL 4 - Model 1 with a symmetric reinforced torpedo loading hatch cutout. A heavy stiffener at the cutout edge was used for reinforcement.	15
15	MODEL 5 - An external ballast tank added to Model 1, with fully fixed bulkheads at each end and intermediate struts to the pressure hull.	16
16	MODEL 6 - The full submarine structure including deck, trim tank, hatch cutout and external ballast tank.	16
17	MODEL 7 - The refined grid model for interframe buckling prediction of the geometry of Model 1; the axisymmetric pressure hull alone.	17

18	MODEL 8 - The interframe model for the deck and trim tank of Model 3. The stiffeners in the deck and longitudinal bulkhead were smeared into the plating as in Model 3.	17
19	MODEL 9 - The interframe model for the external ballast tank of Model 5.	18
20	MODEL 10 - The complete interframe model incorporating the pressure hull, deck, trim tank and external ballast tank; similar to Model 6 but without the cutout.	18
21	Finite Element Model of the Forward End of an Oberon Class Pressure Hull and Strain Gauge Locations	19
22	Minimum Overall Buckling Mode of Axisymmetric Pressure Hull from Axisymmetric Analysis-Longitudinal and Circumferential Cross Sections	21
23	Minimum Overall Buckling Mode of Axisymmetric Pressure Hull from Three Dimensional Finite Element Analysis	21
24	Minimum Interframe Buckling Mode of Axisymmetric Pressure Hull from Axisymmetric Analysis-Longitudinal and Circumferential Cross Sections	22
25	Minimum Interframe Buckling Mode of Axisymmetric Pressure Hull from Three Dimensional Finite Element Analysis	22
26	Pressure Hull Stress Contour Pattern of Axisymmetric Pressure Hull - Model 1	23
27	Pressure Hull Stress Contour Pattern of Dent in Pressure Hull - Model 2	25
28	Pressure Hull Stress Contour Pattern of Deck-Trim Tank With Pressure Hull - Model 3	26
29	Pressure Hull Stress Contour Pattern of Cutout in Pressure Hull - Model 4	26
30	Pressure Hull Stress Contour Pattern of Ballast Tank With Pressure Hull - Model 5	27
31	Pressure Hull Stress Contour Pattern of Complete Submarine Section - Model 6	28
32	Minimum Overall Buckling Mode Shape for Dented Pressure Hull - Model 2	29
33	Minimum Overall Buckling Mode Shape for Deck-Trim Tank With Pressure Hull - Model 3	29
34	Minimum Overall Buckling Mode Shape for Cutout in Pressure Hull - Model 4	30
35	Minimum Overall Buckling Mode Shape for Ballast Tank With Pressure Hull - Model 5	30
36	Minimum Overall Buckling Mode Shape for Complete Submarine Section - Model 6	31
37	Minimum Interframe Buckling Mode Shape for Deck-Trim Tank With Pressure Hull - Model 8	32
38	Minimum Interframe Buckling Mode Shape for Ballast Tank With Pressure Hull - Model 9	32
39	Minimum Interframe Buckling Mode Shape for Complete Submarine Section - Model 10	33

Notation

<i>E</i>	Young's modulus
<i>E_t</i>	tangent modulus for strain hardening
<i>I_c</i>	moment of inertia of frame and shell section
<i>L</i>	length of cylinder between rigid ends
<i>L_f</i>	length of shell between stiffeners
<i>n</i>	circumferential wave number for buckling
<i>P_{ci}</i>	interframe bifurcation buckling collapse pressure
<i>P_{co}</i>	overall bifurcation buckling collapse pressure
<i>r</i>	radius of cylindrical shell
<i>t</i>	thickness of shell
<i>v</i>	Poisson's ratio
<i>λ</i>	$\frac{\pi r}{L}$
<i>σ_y</i>	yield stress of material

1 Introduction

In general, submarine primary structure consists of axisymmetric ring stiffened cylinders, cones, and dome endcaps, which are the most efficient pressure hull structural configurations to withstand large hydrostatic pressures. Primary structural analysis of submarines can be greatly simplified by studying only the idealized axisymmetric pressure hull. Uniformly stiffened cylinders can be analyzed with simplified equations resulting from closed form solutions, while more complex axisymmetric geometries can utilize efficient computer codes for structural analysis of shells of revolution. Variation from this idealized structure occurs with the inclusion of decks and tanks welded to the inner and outer pressure hull surfaces (Figure 1). Hull penetrations of various sizes and fabrication imperfections and/or dents acquired during service may further detract from axisymmetry. This additional secondary structure can be analyzed separately from the primary pressure hull to verify its own integrity; however, there may be significant interaction between the secondary structure and the primary pressure hull inducing varying degrees of asymmetry, thereby bringing into question the validity of an axisymmetric analysis. The problem addressed in this report is the determination of the similarities and differences between results from complex and simplified analysis methods and the determination of the effects of structural variation from axisymmetry on the global stress and stability behaviour of the pressure hull.

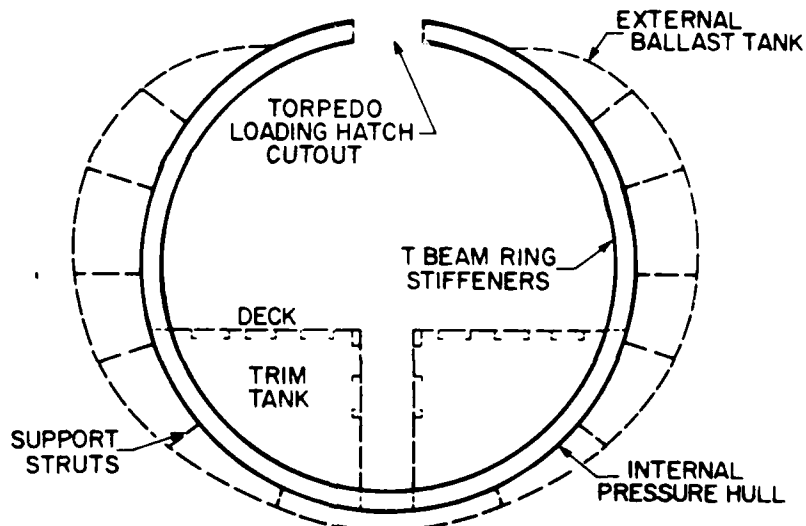


Figure 1: Cross Section of Submarine Geometry

Submarine structural analysis is based on determining the load at which yield occurs and the loads at which elastic bifurcation buckling occur. Since buckling is a catastrophic failure mode, submarines are designed to first reach plastic collapse loads with theoretical elastic buckling loads occurring well above the yield load of the structure. The primary loading function is external hydrostatic pressure which includes loading on the endcaps as well as on the cylindrical portion of the hull. Typical safety factors on the maximum design operating pressure are 1.5 for yielding, 2.5 for interframe elastic bifurcation buckling (Figure 2) and 3.5 for overall elastic bifurcation buckling (Figure 3). The relationship of the three failure modes is shown in Figure 4, which represents a typical pressure load versus generalized displacement curve for a pressure hull.

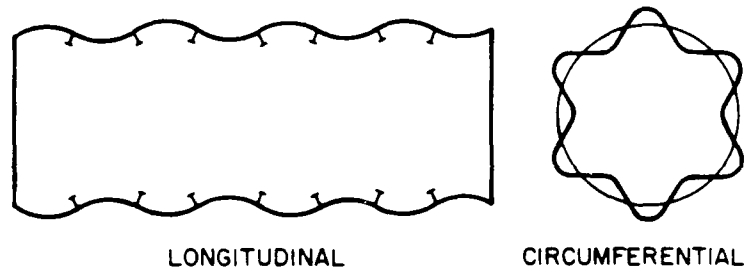


Figure 2: Interframe Elastic Bifurcation Buckling Mode Shape of A Ring Stiffened Cylinder

Considerable experimental work has indicated that, in general, theoretical collapse pressures are too high. Imperfections in the hull geometry (out of roundness due to construction methods), particularly in modes resembling elastic buckling modes, cause interaction between the plastic yield and interframe buckling modes resulting in lower collapse pressures than theory can predict. Design codes compensate for this by incorporating experimental data in establishing collapse loads [1]. This study is concerned with determining the theoretical collapse pressures which are used in the design code methods.

Three levels of analysis, categorized as to their complexity and flexibility, can be used in submarine structural analysis. Predictions of stress, elastic bifurcation buckling and collapse loads from the three levels of analysis are presented and compared. The first level involves closed

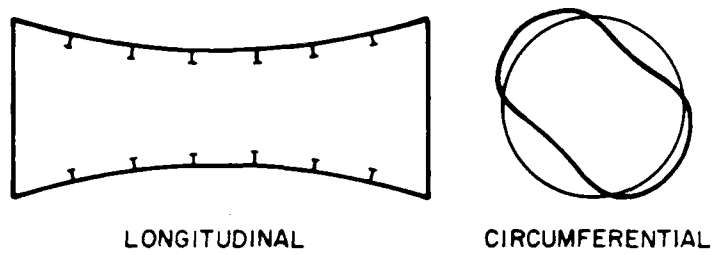


Figure 3: Overall Elastic Bifurcation Buckling Mode Shape of A Ring Stiffened Cylinder

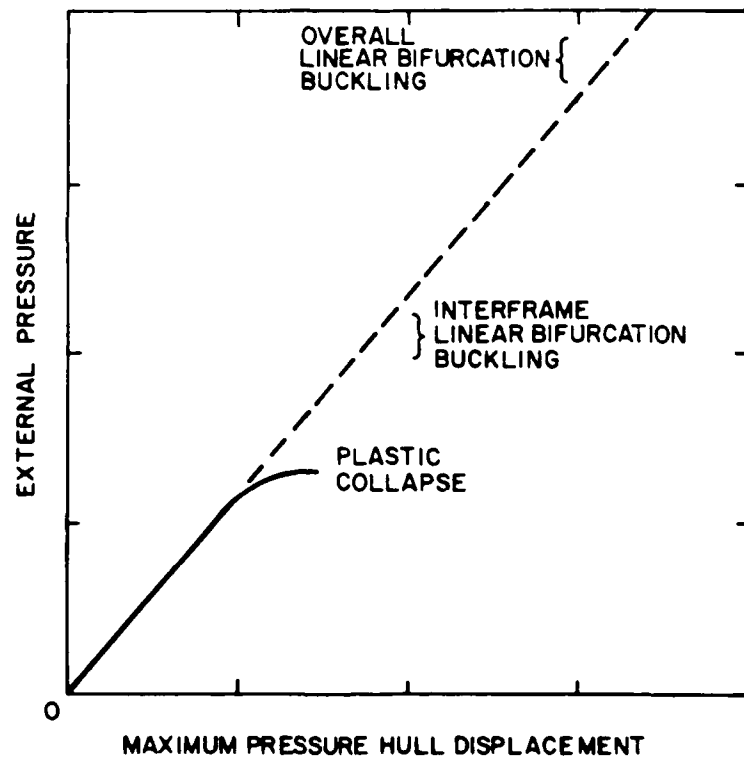


Figure 4: Deflection vs Load Relationship of Three Failure Mechanisms

form, equation based solutions for constant diameter, uniformly stiffened and uniformly loaded cylinders. The second level covers finite difference and finite element analysis methods for complex axisymmetric geometries. The third level is three dimensional finite element analysis which incorporates the complete structure including asymmetric structure and loading. Figure 5 illustrates the structural type and loading which each category of analysis can incorporate.

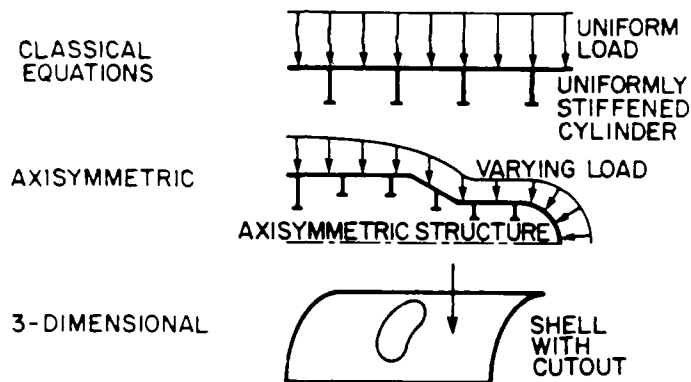


Figure 5: Three Categories of Analysis Methods

Finite element programs provide the option to perform detailed analysis of complete structures without major simplification of complex geometry; however, modelling an entire submarine structure to the detail necessary to predict stress distributions and interframe bifurcation buckling is a prohibitively complicated and costly task. It is also difficult to establish credibility in results for complicated finite element models particularly in determining buckling or collapse loads which may appear to occur through numerical rather than structural instabilities. Thus simplified methods of analysis which assume an axisymmetric pressure hull alone remain a very attractive and necessary part of the design process.

To investigate the effects of secondary structure on the axisymmetric pressure hull structural

behaviour, a short section of pressure hull which is fundamentally axisymmetric, cylindrical and uniformly stiffened was modelled. A large cutout opening, deck and trim tank plating, an external ballast tank and a large dent were then incorporated into the pressure hull model separately and in combination to assess their influence on the axisymmetric pressure hull behaviour. The section was that of Figure 1 extended over 6 frames and bounded on each end by a rigid bulkhead. The configuration used was similar to the Oberon class hull but dimensions were altered to simplify model creation and exemplify specific behaviour.

In parallel with the present study, to further assess axisymmetric characteristics of a pressure hull, an attempt was made to measure strains around the circumference of an Oberon class submarine hull. Unfortunately, limited access to the pressure hull and moisture problems prohibited the placement of strain gauges over all but a small portion of the circumference so that stress results for the full cross section were not attainable. The section of the pressure hull which was accessible for strain gauge application was not axisymmetric.

2 Criteria for Pressure Hull Strength

As previously mentioned, the analysis of submarine structures involves the determination of yield collapse through investigating the stress state in the structure and the determination of overall and local buckling instability loads. A brief discussion of these collapse mechanisms for the specific case of ring stiffened cylinders is given here.

2.1 Stress in Ring Stiffened Cylinders

The stress state in the shell of a ring stiffened cylinder subject to hydrostatic pressure consists of three superimposed principal actions:

1. circumferential membrane compression,
2. axial membrane compression, and
3. bending between stiffeners or bulkheads.

The regions of maximum stress in the shell resulting from the above actions are (Figure 6):

1. at the outer surface of the shell at midbay between stiffeners, and
2. at the inner surface of the shell at the shell stiffener connection.

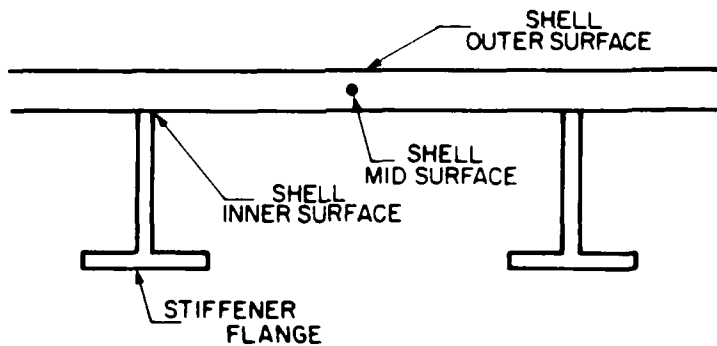


Figure 6: Critical Stress Points in A Ring Stiffened Cylinder

The attainment of the yield limit at these locations does not lead to failure[2] since the development of a collapse hinge mechanism does not occur until yield progresses further into the shell cross section. For this reason, the mean circumferential stress value at the mid surface of the shell cross section at midbay between stiffeners is often used as the failure criterion.

Failure is deemed to occur when this stress value exceeds yield. When the stress value at the shell surface is used as the limiting value, the Hencky-Von Mises strain energy criterion is often used to determine failure as it allows a higher load limit and gives the best agreement with experimental results.

The stress state in the ring stiffener is one of combined circumferential compression and bending. The maximum stresses in the web and the outer fiber of the flange are of interest. These stress values are used to determine both plastic collapse loads and local instability limits of the ring stiffener.

The stress state in an axisymmetric ring stiffened cylinder subject to uniform hydrostatic pressure is axisymmetric. The inclusion of secondary structure will cause local deviations to this axisymmetric pattern. This study investigates the extent of these deviations.

2.2 Buckling Stability of Ring Stiffened Cylinders

Any structure subject to compressive loading is susceptible to instability. Bifurcation buckling instability occurs when membrane compression energy is suddenly converted into bending energy in a structural configuration which cannot withstand significant bending action. Thin shells subject to external pressure are of this class of structure.

Three types of instability can occur in ring stiffened pressure vessels subject to external hydrostatic pressure:

1. overall buckling: where the shell and stiffeners fail as one unit forming a half sine wave between bulkhead or supported ends and 2 to 6 waves circumferentially (Figure 2),
2. interframe buckling: where the rings remain essentially undeformed and the intermediate shell forms half sine waves between stiffeners and 10 to 20 waves circumferentially (Figure 3), and
3. frame buckling: where the ring frame undergoes lateral torsional buckling (tripping) or local crippling of the web or flange (Figure 7).

The first two modes of failure are considered in this study. The third can usually be prevented by proper stiffener dimensioning and is not considered further here.

The buckling load is dependent on the stress state in the cylinder. The axisymmetric pressure hull alone will produce uniform sinusoidal buckling modes. The addition of secondary structure which produces localized changes in the stress distribution can be expected to effect the buckling loads and mode shapes.

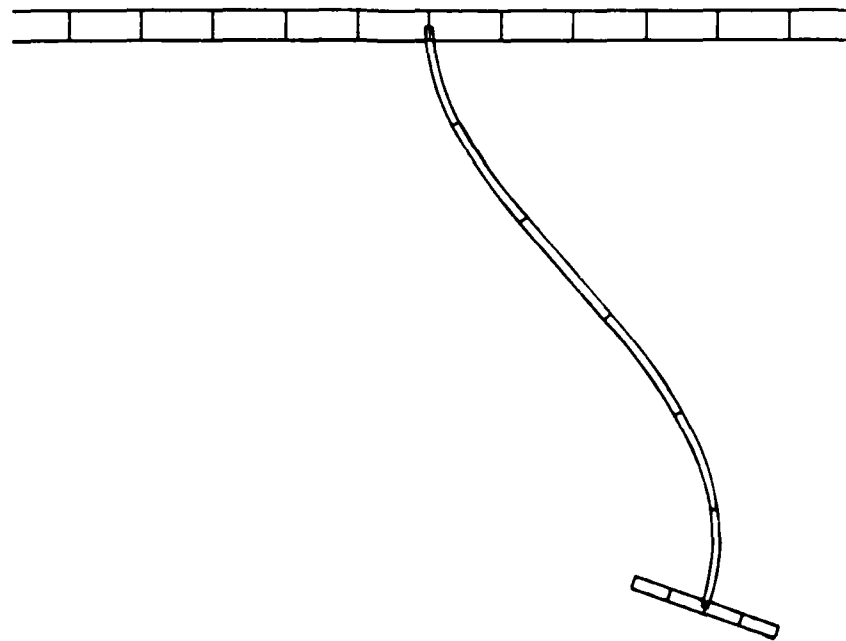


Figure 7: Frame Buckling Failure Mode

3 Analytical Solution Methods

As described in the introduction, three levels of analyses were studied and compared. Each level was progressively more flexible in the type of problem it could solve, at a cost of increased complexity and effort. All three levels are used in modern submarine design and play an important role in determining stress and structural stability characteristics. Full scale three dimensional finite element analysis, particularly nonlinear, is still primarily used as a specialty research tool.

3.1 Equation Based Solutions

Approximate closed form solutions for the stress distribution and bifurcation buckling loads of constant diameter, uniformly stiffened cylinders have been derived by several researchers[2,3,4]. Some of these equation based solutions have been programmed[5] and used in this study. Cylinders with moderately varying stiffener spacing and dimensions may be analyzed with these equations by using average stiffener geometry.

The stress values described in section 2.1 were determined by the equations of references 2 or 3. These are solutions of the differential equation for uniformly loaded ring stiffened cylinders and are described and programmed for solution in reference 5.

Von Mises' solution to the differential equation for radial displacement in unstiffened cylinders, as modified by Kendrick[2], has given good predictions for interframe buckling of stiffened cylinders:

$$P_c = \frac{Et}{r} \frac{1}{[n^2 - 1 + \frac{1}{2}(\frac{\pi r}{L_f})^2]} \left\{ \frac{1}{[n^2(\frac{L_f}{\pi r})^2 + 1]^2} + \frac{t^2}{12r^2(1 - \nu^2)} [n^2 - 1 + (\frac{\pi r}{L_f})^2] \right\}$$

Bryant developed a well accepted solution for overall buckling which combines the buckling load for an unstiffened shell with that of a single segment of shell and stiffener to give the total buckling load[2]:

$$P_c = \frac{(\frac{Et}{r})\lambda^4}{(n^2 - 1 + \frac{\lambda^2}{2})(n^2 + \lambda^2)^2} + \frac{(n^2 - 1)EI_c}{r^3 L_f}$$

Lunchick developed a method for predicting the plastic axisymmetric collapse load of uniformly stiffened cylinders using the Hencky-Von Mises yield criterion[4]. He has shown that this gives the best prediction relative to experimental data. This method, programmed in reference 6, was used in this study.

3.2 Axisymmetric Analysis

Equation based methods are limited to uniformly stiffened cylinders and so are applicable only to select structures or parts of structures. The main structure of a submarine hull, while

not necessarily cylindrical, is usually axisymmetric in geometry. Several computer codes exist for the stress, vibration, buckling and collapse analysis of complex shells of revolution. The axisymmetric methods give numerical approximations for stress and stability loads. The structure is mathematically described by discretizing it into small sections; the more sections the more accurate the result. The discretization process leads to the formation of matrix equations easily solved by computer. An axisymmetric model representing a submarine as a single meridian of the structure is shown in Figure 8. Two different axisymmetric analysis methods have been used at DREA for pressure hull studies: finite difference and finite element.

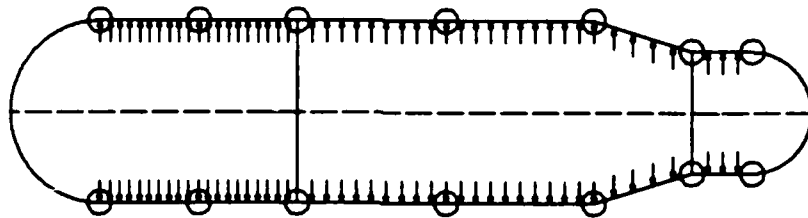


Figure 8: Axisymmetric Model of A Typical Submarine Pressure Hull

3.2.1 Axisymmetric Finite Difference Analysis

The BOSOR4[7] and BOSOR5[8] finite difference programs, initially developed for aerospace applications, have been found to be excellent tools for axisymmetric stiffened shell analysis. BOSOR4 has been used to determine the elastic stress and stability characteristics of the axisymmetric pressure hull. For this study, the finite difference model was formed from six evenly spaced nodes between each of six stiffeners. The stiffeners were modelled as eccentric discrete rings. BOSOR5 is a nonlinear extension of BOSOR4 and was used to determine the collapse loads in the plastic regime by tracking displacements to the point of stiffness matrix singularity.

3.2.2 Axisymmetric Finite Element Analysis

The DND finite element code VAST[9] has a specialized axisymmetric analysis component. Pre and post processors designed specifically for VAST submarine pressure hull analysis have been developed. VAST offers capabilities similar to the BOSOR programs with a greater range of static and dynamic load options and the capability to include the surrounding fluid, which is

important for submarine dynamic analysis. The formulations of axisymmetric finite elements are often similar to their three dimensional counterparts which allows an economical exploration of grid layout before creating full three dimensional models. The finite element model had five 3 noded axisymmetric shell elements between stiffeners which were modelled as eccentric discrete axisymmetric beam elements (Figure 9).



Figure 9: Axisymmetric Finite Element Model of the Pressure Hull Section

3.3 Three Dimensional Analysis

The inclusion of the deck, tanks, cutout, and dent resulted in the loss of axisymmetry in the structure. It was therefore necessary to use three dimensional finite element methods to determine the stress and stability characteristics of these models. In some cases, such as the Oberon class submarine, parts of the pressure hull are not axisymmetric, and require generalized three dimensional analysis methods.

The effort required in the three dimensional analysis was several orders of magnitude greater than in the axisymmetric analysis. Potential for error was also considerably greater and predictions from the simpler methods were necessary to give confidence in the three dimensional results. Choosing the proper finite element mesh layout is crucial: buckling modes may be missed in poorly constructed meshes.

3.3.1 Linear Analysis

VAST was used for determining the linear stress and bifurcation buckling loads of the three dimensional models. Specialized model generating programs were developed and employed to generate the pressure hull, decks and tanks and connect them together. Buckling eigenvalues are calculated in the usual way by forming an elemental geometric stiffness matrix based on the stress distribution from a unit load. The load multipliers which result in the determinant of the combined structural and geometric stiffness matrices becoming zero are the buckling eigenvalues.

3.3.2 Nonlinear Analysis

The finite element program, ADINA [10], was used to determine the nonlinear, plastic collapse load of the various models. Both material and large displacement geometric nonlinearities were modelled. Load steps were varied to narrow in on the collapse load, which was taken as the load point at which matrix instability occurred. A bilinear material model was used in the analysis with parameters: Young's modulus = 207,000 MPa; yield stress = 430 MPa; and tangent modulus = 70 MPa (Figure 10).

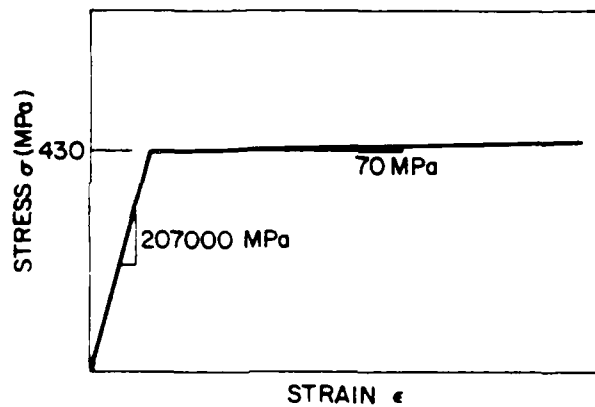


Figure 10: Stress Strain Material Curve Used in Nonlinear Analysis

3.3.3 Three Dimensional Finite Element Structural Models

A total of ten different geometric models ranging from the axisymmetric pressure hull alone to the full section including pressure hull, cutout, deck, trim tank, and external ballast tank (Figure 1) were investigated. Rigid bulkheads were placed at the ends, and symmetry about the centerline vertical axis was used. Variations in grid layout were studied to ensure consistent results. Preliminary investigation indicated that the minimum interframe buckling load occurred with a mode shape involving 12 to 15 circumferential sine waves. To accurately model the large gradients in the displacements of this mode required considerably more elements in both the circumferential and longitudinal directions than for the overall half sine wave mode. To achieve this efficiently, separate models incorporating a single stiffener with attached shell segment

were used to investigate the interframe modes. The same models were used for the linear and nonlinear analyses.

The finite element models for predicting the overall half sine wave buckling load (Models 1-6) have two 8 noded isoparametric shell elements between stiffeners and eight elements around half the circumference. The stiffeners are modelled using compatible, three noded, isoparametric, eccentric, beam elements. The finite element models used to determine the interframe buckling loads (Models 7-10) have four elements between stiffeners and thirty elements around half the circumference. The model specifications are given in Figures 11 to 20.

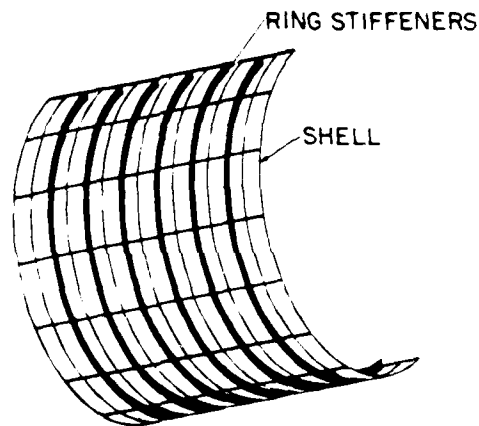


Figure 11: MODEL 1 - A three dimensional half model of a length of axisymmetric pressure hull between bulkheads, with shell plating and six T-bar stiffeners.

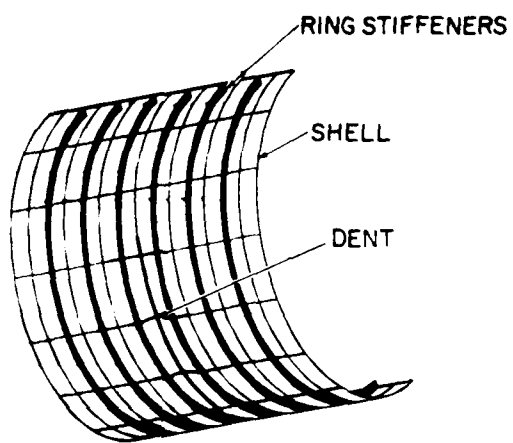


Figure 12: MODEL 2 - Model 1 with a large dent modelled between two stiffeners on the side of the pressure hull. The dent is sinusoidal in shape with a maximum depth equal to the frame depth and a half period equal to the length between stiffeners.

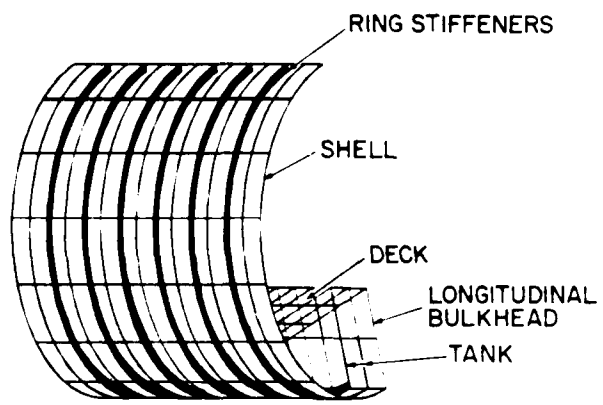


Figure 13: MODEL 3 - Model 1 with the trim tank added which consisted of a deck on top and a vertical bulkhead on its side. The deck and bulkhead stiffeners were modelled by smearing them into equivalent plating.

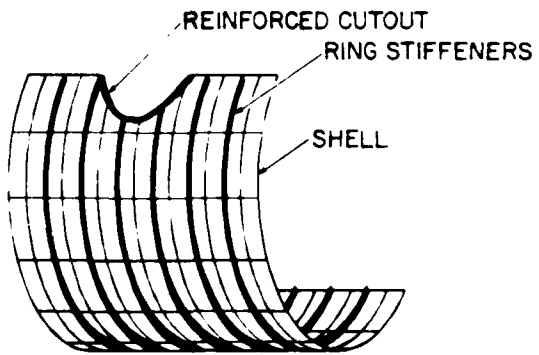


Figure 14: MODEL 4 - Model 1 with a symmetric reinforced torpedo loading hatch cutout. A heavy stiffener at the cutout edge was used for reinforcement.

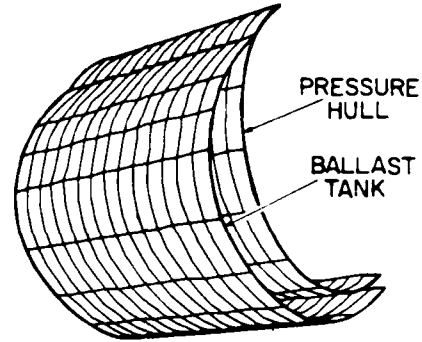


Figure 15: MODEL 5 - An external ballast tank added to Model 1, with fully fixed bulkheads at each end and intermediate struts to the pressure hull.

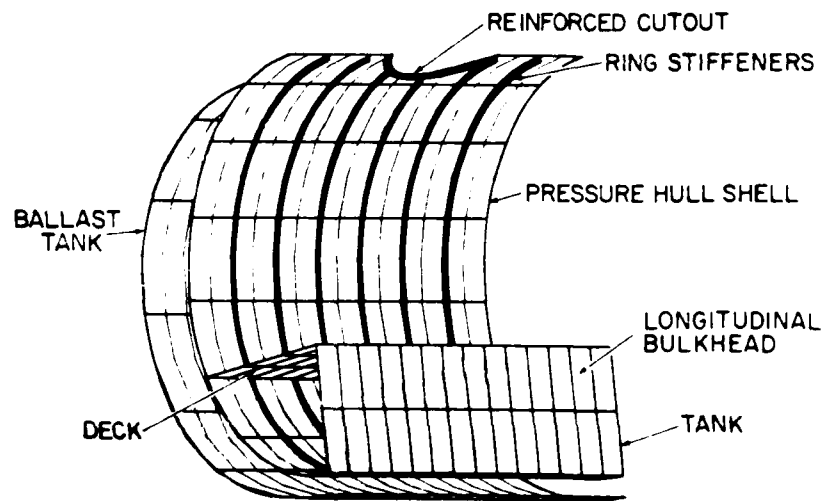


Figure 16: MODEL 6 - The full submarine structure including deck, trim tank, hatch cutout and external ballast tank.

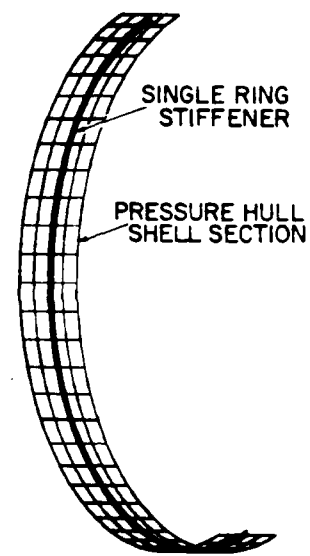


Figure 17: MODEL 7 - The refined grid model for interframe buckling prediction of the geometry of Model 1; the axisymmetric pressure hull alone.

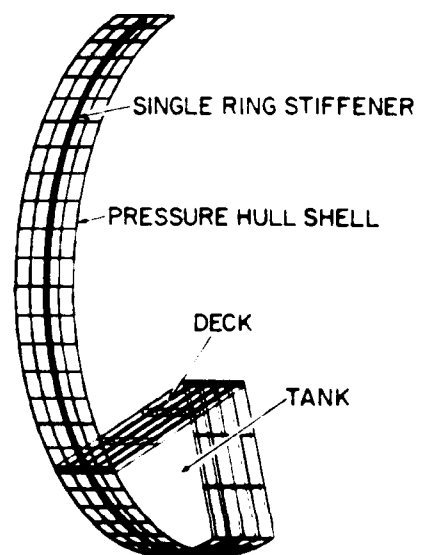


Figure 18: MODEL 8 - The interframe model for the deck and trim tank of Model 3. The stiffeners in the deck and longitudinal bulkhead were smeared into the plating as in Model 3.

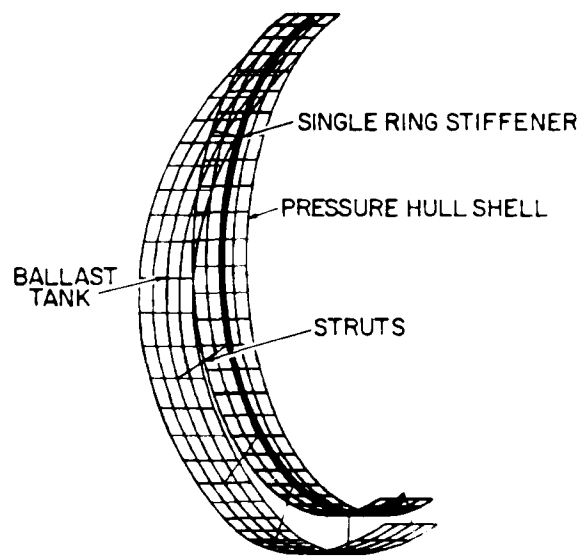


Figure 19: MODEL 9 - The interframe model for the external ballast tank of Model 5.

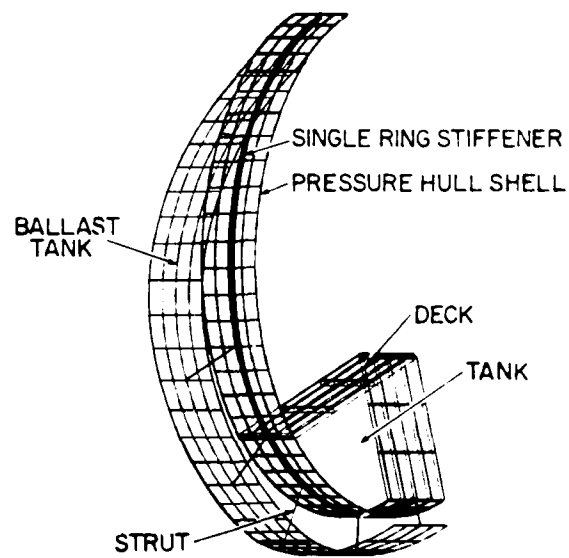


Figure 20: MODEL 10 - The complete interframe model incorporating the pressure hull, deck, trim tank and external ballast tank; similar to Model 6 but without the cutout.

4 Experimental Strain Measurements

To investigate the axisymmetric stress behaviour in a pressure hull it was initially proposed to place strain gauges around the entire circumference of one cross section of an Oberon class submarine; however, a strain gauge pattern covering 360 degrees could not be attained. The inaccessibility of the pressure hull and excessive condensation on the metal below the waterline limited the area covered to approximately 40 degrees. The most accessible region of the hull was at the forward end just aft of the torpedo tubes, between frames 20 and 21. This part of the pressure hull was not axisymmetric as it has a straight top meridian and upward sloping bottom meridian at this location (Figure 21). Thus, an axisymmetric stress distribution could not be determined; however, sufficient data were taken to estimate the general trend of the stress distribution in this area and compare it to finite element stress results.

Strain gauges were located at three angular locations as indicated in Figure 21 at 70, 60 and 30 degrees from the top meridian of the pressure hull. Strains were measured on the shell midway between stiffeners in the circumferential direction for locations A and C and in both circumferential and axial directions at location B. Rosettes were used to measure principal strains in the flange and the web shell connection region. Only the shell data were used for this study.

Strain readings were taken at equal depth intervals while submerging and again while surfacing. The boat was held as close to constant depth as possible while readings were manually recorded.

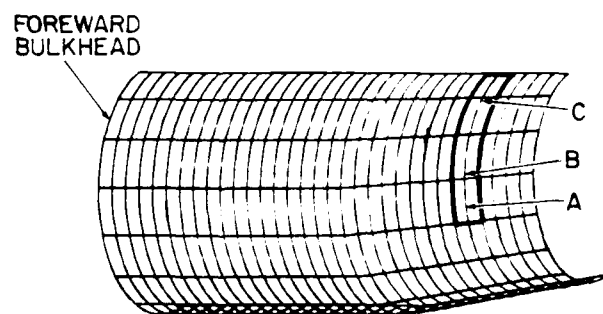


Figure 21: Finite Element Model of the Forward End of an Oberon Class Pressure Hull and Strain Gauge Locations

5 Results and Discussion

5.1 Comparison of Methods for Axisymmetric Pressure Hull Analysis

Four solution methods were applied to the axisymmetric pressure hull buckling analysis: equation based, finite difference, axisymmetric finite element and three dimensional finite element. Results are summarized in Table 1. The results are nondimensionalized with respect to the results of the Bryant formula, the Von Mises formula and Lunchick's method for the overall buckling, interframe buckling and collapse loads respectively.

		Linear			Nonlinear		
	Equation Based	BOSOR4 Axisymm	Fin Elem Axisymm	Fin Elem 3D	Equation Based	BOSOR5	ADINA
Overall Buckling Load	1.0(4) ^a	0.89(4)	0.93(4)	0.93(4)			
Interframe Buckling Load	1.0(15) ^b	1.13(15)	1.13(15)	1.09(12)			
Max Midbay Circ. Stress	1.0	0.95	0.95	0.95			
Plastic Collapse Load					1.0 ^c	1.03	1.03

^a Bryant formula², numbers in brackets are circumferential wave number

^b Kendricks modified Von Mises formula²

^c Lunchick formula³

Table 1: Comparison of Predictions for Axisymmetric Pressure Hull Alone Nondimensionalized to Equation Based Solutions

There is an 11 percent variation in the minimum overall buckling load determination but all methods give the same circumferential wave number, 4. The lowest overall buckling mode for the axisymmetric pressure hull is shown in Figures 22 and 23 for the finite element axisymmetric and three dimensional models respectively. The longitudinal half sine wave and four circumferential waves are clearly seen in both models (only two waves can be seen in the figure as this is a half model due to the use of lateral symmetry). The Bryant formula gives higher buckling loads than the numerical solution methods primarily because it does not account for the membrane shearing effects caused by the interframe deflection and rigid end effects. This unconservative behaviour reduces as the cylinder length increases.

The values obtained for the minimum interframe buckling loads for the axisymmetric hull vary by 13 percent. The lowest interframe buckling mode for the pressure hull is shown in Figures 24 and 25 for the finite element axisymmetric and three dimensional models respectively.

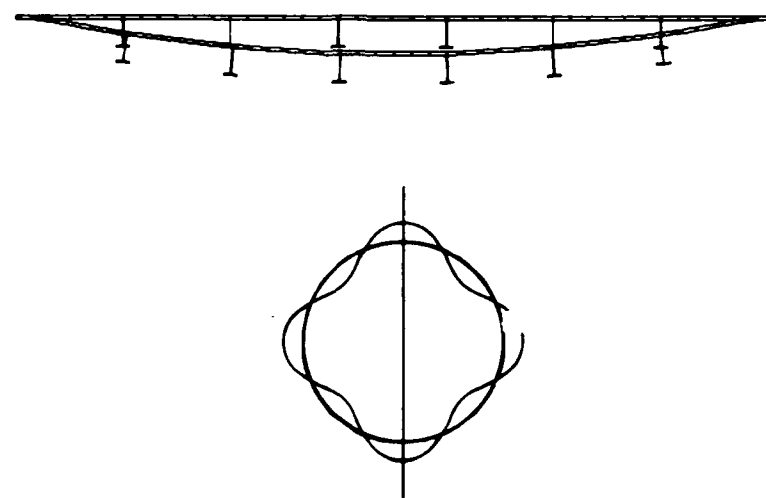


Figure 22: Minimum Overall Buckling Mode of Axisymmetric Pressure Hull from Axisymmetric Analysis-Longitudinal and Circumferential Cross Sections

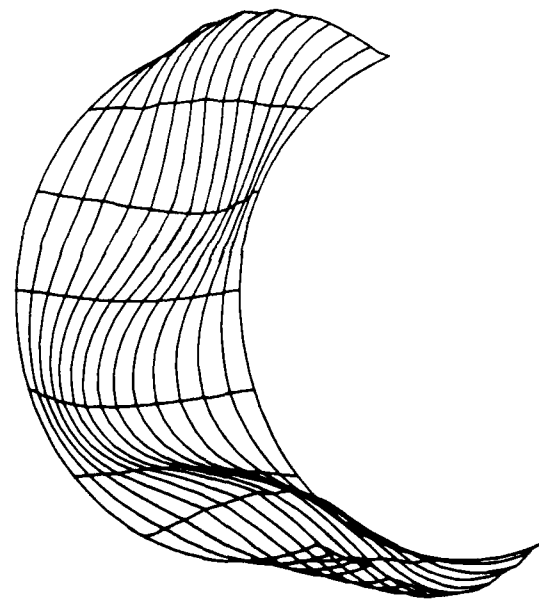


Figure 23: Minimum Overall Buckling Mode of Axisymmetric Pressure Hull from Three Dimensional Finite Element Analysis

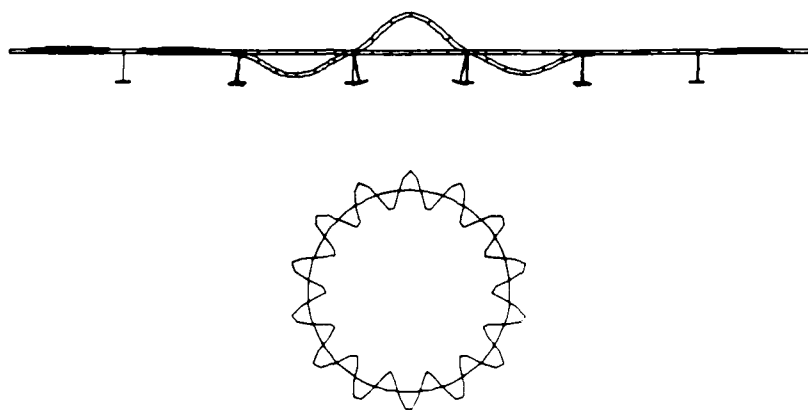


Figure 24: Minimum Interframe Buckling Mode of Axisymmetric Pressure Hull from Axisymmetric Analysis-Longitudinal and Circumferential Cross Sections

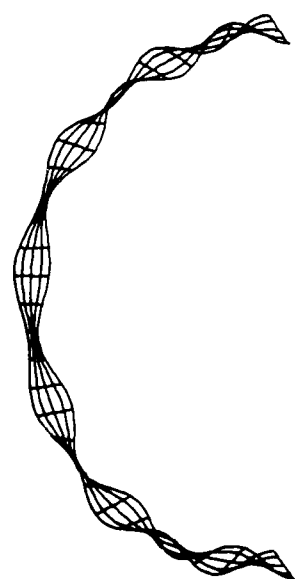


Figure 25: Minimum Interframe Buckling Mode of Axisymmetric Pressure Hull from Three Dimensional Finite Element Analysis

All three numerical solutions predicted clusters of buckling loads in the 10 to 16 circumferential wave range with little difference in the buckling load values. For this case, small differences in modelling can shift the wave number up or down without significant change in the minimum buckling load. The modified Von Mises buckling load, as expected, gives lower results as it assumes a simply supported section of shell between stiffeners whereas some rotational stiffness at the frame connection is realized in the numerical solutions.

The midbay circumferential stresses agree well. Stress values for an applied unit pressure load are given in Table 1. Figure 26 shows the axisymmetric stress pattern in the three dimensional finite element model. This is a contour plot which shows variation longitudinally in the region of the end bulkheads and stiffeners and does not vary in the circumferential direction.

The nonlinear collapse load predictions of BOSOR5, ADINA, and the Lunchick equation compare well for the axisymmetric hull. The numerical solutions indicated that failure began through yielding at the shell bulkhead connections, quickly followed by yielding throughout the shell in the circumferential and axial directions. The stiffeners were modelled as equivalent rectangular discrete sections; thus, local yielding and instability could not be predicted. The average compressive stress in the stiffeners was found to be about 85 percent of the stress at midbay in the shell. Both the shell and beam elements used in ADINA were formulated using Von Mises' yield criterion and have isotropic strain hardening[10]. The actual value of the collapse load derived from ADINA and BOSOR5 is taken as the point where deformations increase rapidly with small load increase, causing singularities to occur in the stiffness matrix.

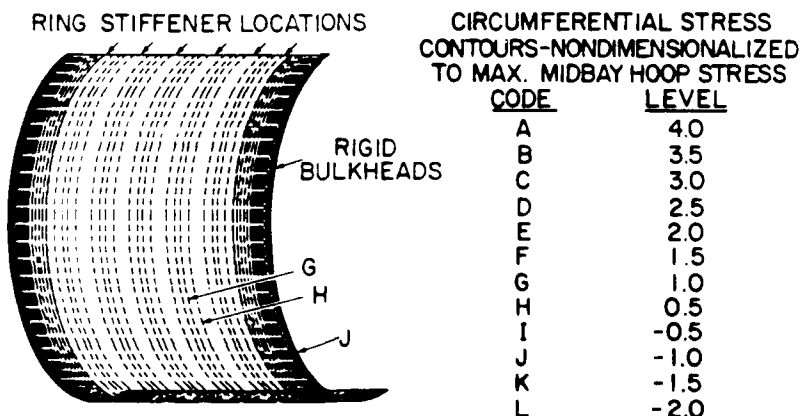


Figure 26: Pressure Hull Stress Contour Pattern of Axisymmetric Pressure Hull - Model 1

5.2 Comparison of Three Dimensional Models with Secondary Structure

The results of the models including secondary structure showed significant variation from those obtained by axisymmetric analysis. Table 2 summarizes buckling, stress and collapse load results for the ten different geometric models; again the results are nondimensionalized with respect to the Bryant, Von Mises, and Lunchick load values for the overall buckling, interframe buckling, and collapse loads, respectively. Percentage comparisons are made with respect to the three dimensional results of the axisymmetric pressure hull alone (column 1).

	MODEL1+7 Axisymm	MODEL2 Dent	MODEL3+8 Trim Tank	MODEL4 Cutout	MODEL5-9 Ballast Tank	MODEL6-10 Full Sub
Overall Buckling Load	0.93(4)	0.72(4)	0.99(4)	0.88(5)	0.96(5) ^a	0.95(4)
	0%	-22%	6%	-5%	3%	5%
Interframe Buckling Load	1.03(12)		1.5(12)		1.46(13)	1.48(13)
	0%		37%		34%	36%
Max Circumferential Stress	0.95	4.2	1.18	2.60	1.06	2.11
	0%	342%	24%	173%	11%	122%
Plastic Collapse Load (ADINA)	1.03	0.76	1.03	0.81	1.03	
	0%	-26%	0%	-21%	0%	

^a ballast tank buckled at a load 14 % lower than the pressure hull

Table 2: Comparison of Predictions for Secondary Structure on Pressure Hull Nondimensionalized to Equation Based Solutions

5.2.1 Stress Results

The inclusion of the secondary structure caused significant variation in the axisymmetric stress values and pattern of Figure 26. Results for the maximum circumferential stresses in the pressure hull are given in the third line of Table 2. Stress values are nondimensionalized with respect to maximum midbay circumferential stress in the axisymmetric model predicted by the equation method.

The circumferential stress pattern resulting from the three dimensional finite element analysis of the dented model (Model 2) is shown in Figure 27. A considerable increase in the bending stresses in the shell resulted from the dent. The maximum stress at midbay in the shell was 342 % greater than the maximum circumferential stress at midbay in the axisymmetric model (Models 1 and 7). The size of this dent was somewhat exaggerated over what may occur in

practice; however, this illustrates the severity of the effects that a dent would have on the shell stress. The residual stress resulting from the formation of the dent was not included in this study.

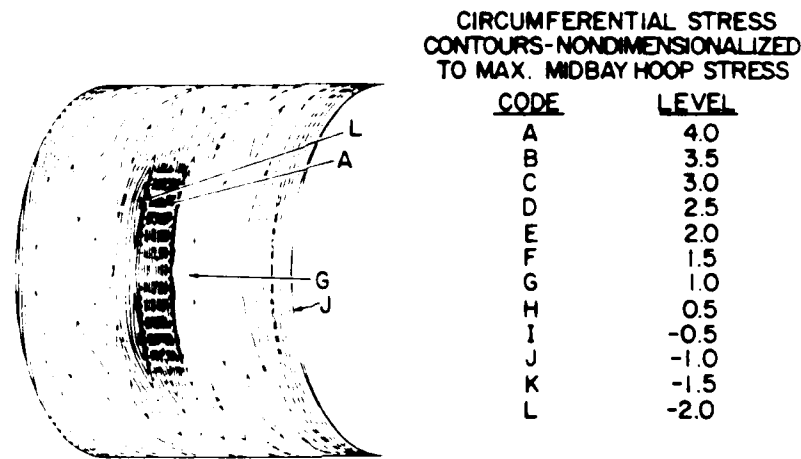


Figure 27: Pressure Hull Stress Contour Pattern of Dent in Pressure Hull - Model 2

The circumferential stress for the model including the deck and trim tank (Model 3) is shown in Figure 28. The deck connection acts as a hard point boundary for the shell. The compression stress on the outer shell surface at the deck intersection is reduced as a result of the bending induced at the connection. Compression stresses increase a short distance from the deck with a 24 % increase in the circumferential stress at midbay at the outer surface of the shell. There was some increase in stress at the bulkhead shell connection below the deck level.

The circumferential stress pattern for the pressure hull with the torpedo loading hatch cutout (Model 4) is shown in Figure 29. There was a significant increase of 173 % in the maximum stress value over the axisymmetric model. This increase appears to be very localized as indicated by the tightly spaced contour lines. The model included a large reinforcing stiffener surrounding the cutout but did not include inserted reinforcing cross bars or the hatch cover. A much more detailed and refined finite element model of this region would give a better representation of the stress values; however, it is expected that there would be an increase in stress in the cutout vicinity which might have significant impact on the global stress pattern of the submarine section.

The stress pattern for the ballast tank and pressure hull (Model 5) is shown in Figure 30. This is similar to what occurred with the trim tank model with the ballast tank-hull connection

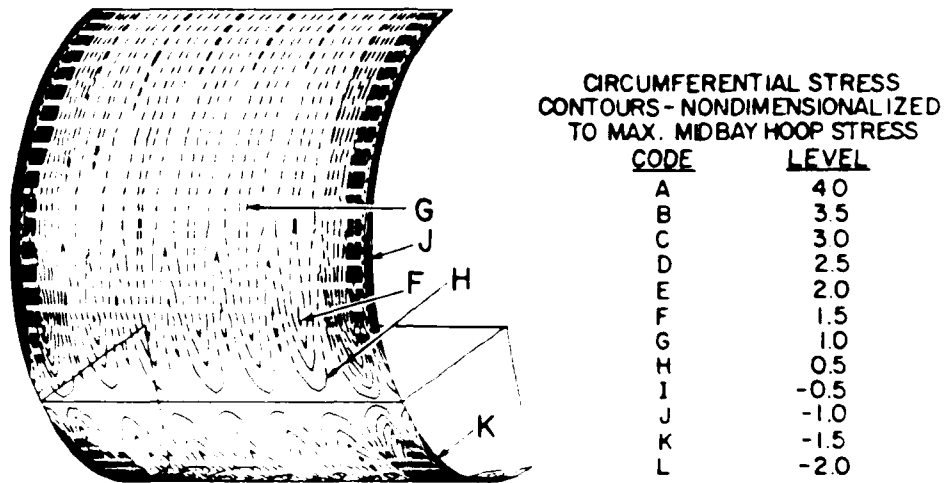


Figure 28: Pressure Hull Stress Contour Pattern of Deck-Trim Tank With Pressure Hull - Model 3

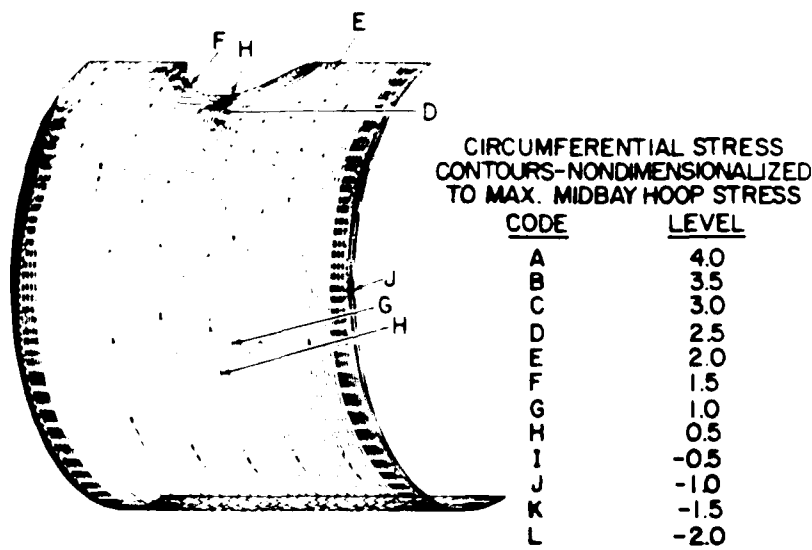


Figure 29: Pressure Hull Stress Contour Pattern of Cutout in Pressure Hull - Model 4

acting as a line of restraint against deformation of the pressure hull. The shell bending about this connection caused a local increase in stress of 11 % in the vicinity of the ballast tank connection.

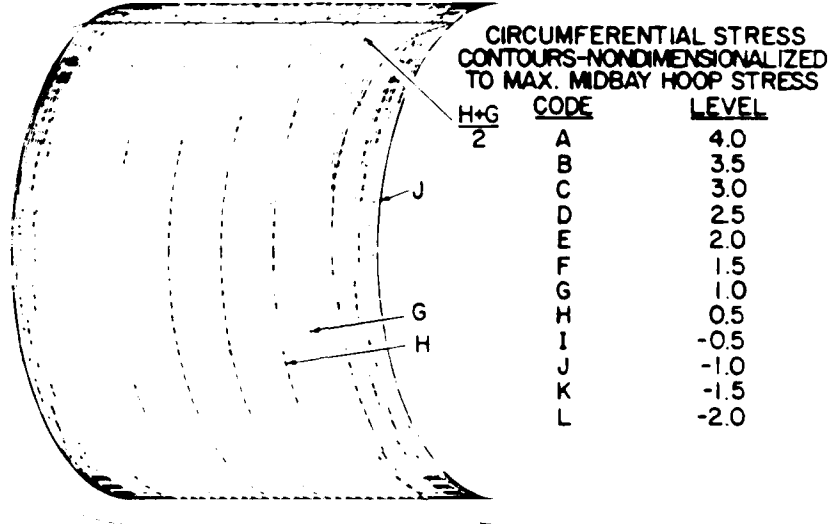


Figure 30: Pressure Hull Stress Contour Pattern of Ballast Tank With Pressure Hull - Model 5

The circumferential stress patterns for the complete structural model (Model 6) is shown in Figure 31. A comparison of Figure 31 with 26 shows the large degree of variation from axisymmetry present in the complete structure. Stress concentrations in the cutout region caused a maximum stress which was 122 % greater than the maximum midbay circumferential stress in the axisymmetric model

5.2.2 Overall Buckling Results

Line one of Table 2 gives the overall buckling load values for the non-axisymmetric three dimensional finite element models including secondary structure.

The lowest overall buckling mode for the dented model (Model 2) is shown in Figure 32. The dent significantly influences the mode shape, as the displacements are much greater in the dented region. The longitudinal half sine wave and four circumferential waves are maintained. The effect of the high bending stresses induced in the dent region was to lower the overall buckling load by 22 % over that of the axisymmetric model.

The lowest overall buckling mode for the deck and trim tank model (Model 3) is shown in Figure 33. The longitudinal half sine wave and four circumferential waves of the axisymmetric

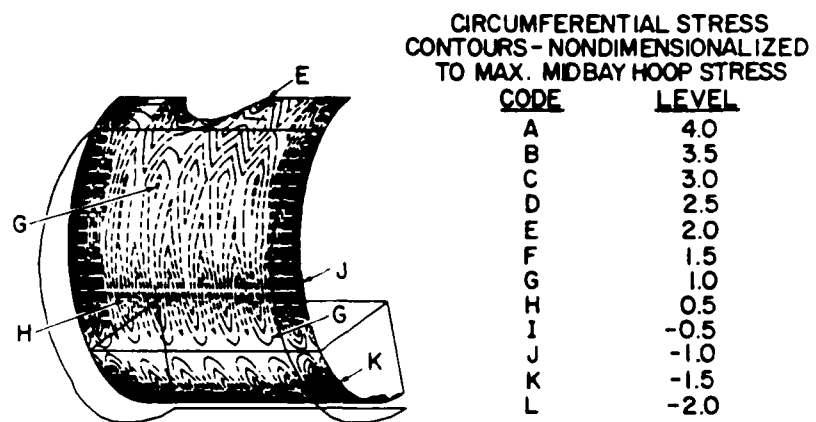


Figure 31: Pressure Hull Stress Contour Pattern of Complete Submarine Section - Model 6

model were maintained; however, the restraint of the deck connection and increased stiffness of the lower portion is evident by the much reduced displacement in this region. This increased stiffness resulted in a 6 % increase in the overall buckling load.

The overall buckling mode for the model with the torpedo hatch cutout (Model 4) is shown in Figure 34. The influence of the cutout is significant as displacements are increased in this region. The longitudinal half sine wave shape was maintained; however, the circumferential wave number increased to 5. The buckling load was reduced by 5 % for this model.

The overall buckling mode shape for the pressure hull and ballast tank combined (Model 5) is shown in Figure 35. The influence of the pressure hull and ballast tank on each other through the attaching struts and upper connecting point is quite interesting. It should be noted here that only the pressure hull was loaded in these analyses and that compression stresses in the ballast tank occur as a result of load transfer from the pressure hull. A buckling load 3 % higher than the axisymmetric case was attained for this model indicating some stiffening effect by the external ballast tank.

The overall buckling mode shape of the complete submarine section model (Model 6) is shown in Figure 36. The amplitude of displacement is greatest in the vicinity of the cutout. The circumferential wave number remained at four. The resulting buckling load was 5 % higher than the pressure hull alone indicating the stiffening effect of the trim tank and ballast tank.

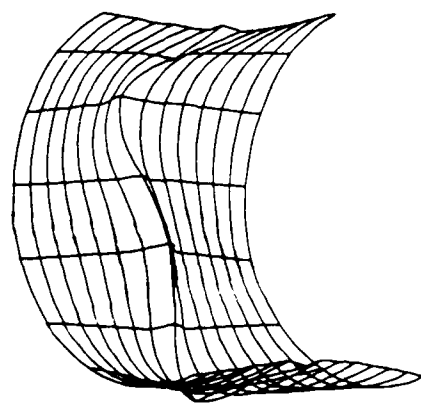


Figure 32: Minimum Overall Buckling Mode Shape for Dented Pressure Hull - Model 2

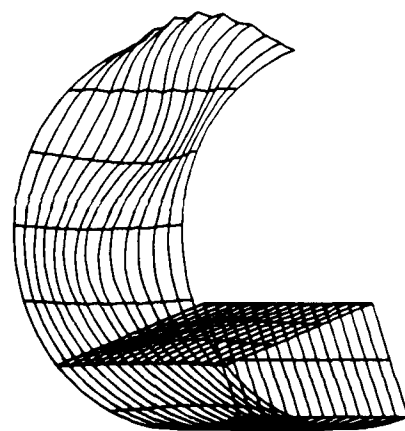


Figure 33: Minimum Overall Buckling Mode Shape for Deck-Trim Tank With Pressure Hull - Model 3

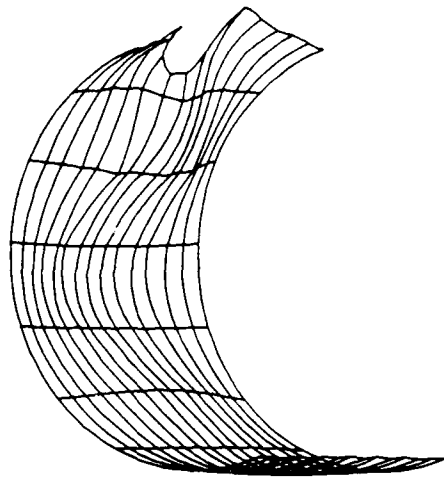


Figure 34: Minimum Overall Buckling Mode Shape for Cutout in Pressure Hull - Model 4



Figure 35: Minimum Overall Buckling Mode Shape for Ballast Tank With Pressure Hull - Model 5

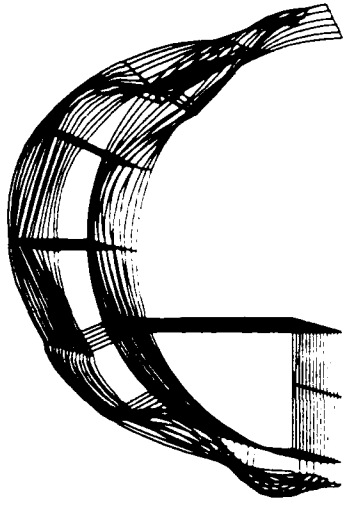


Figure 36: Minimum Overall Buckling Mode Shape for Complete Submarine Section - Model 6

5.2.3 Interframe Buckling Results

Line two of Table 2 gives the interframe buckling load values for the non-axisymmetric three dimensional finite element models.

The mode shape for the minimum interframe buckling load of the deck and trim tank model (Model 8) is shown in Figure 37. When compared to Figure 25, the very significant stiffening effect of the deck-trim tank structure can be seen. Twelve circumferential waves were maintained with the amplitude near and below the deck level greatly attenuated. There was a 37 % increase in the lowest buckling load resulting from the inclusion of the deck and trim tank.

The mode shape for the minimum interframe buckling load of the ballast tank, pressure hull structure (Model 9) is shown in Figure 38. The pressure hull mode shape is quite similar to that of Figure 25 except that there are 13 circumferential waves instead of 12. The ballast tank also shows some displacement resulting from the transfer of compression loading from the pressure hull. The ballast tank's effect was to stiffen the system considerably, resulting in a 34 % increase in the pressure hull buckling load.

The mode shape for the minimum interframe buckling load of the complete structure (Model 10) is shown in Figure 39. The cutout was not included in this model as a detailed model of a larger section would be required to incorporate it. The stiffening effects of the deck-trim tank and ballast tank can be seen. The buckling load was increased 36 % over the axisymmetric

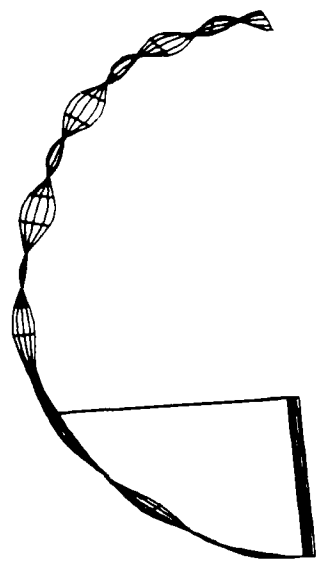


Figure 37: Minimum Interframe Buckling Mode Shape for Deck-Trim Tank With Pressure Hull - Model 8

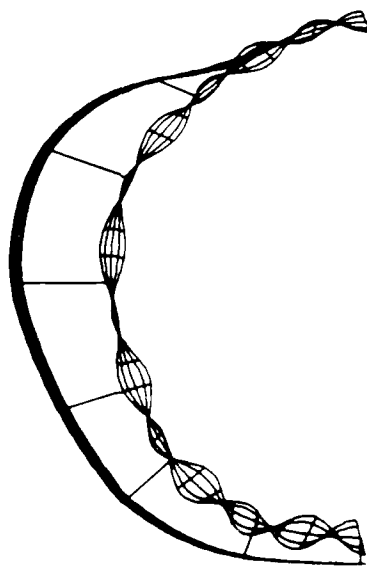


Figure 38: Minimum Interframe Buckling Mode Shape for Ballast Tank With Pressure Hull - Model 9

pressure hull alone. The circumferential wave number was 13. This change in wave number may be caused by the location of the connecting struts of the ballast tank which may influence the node location in the buckling mode shape.

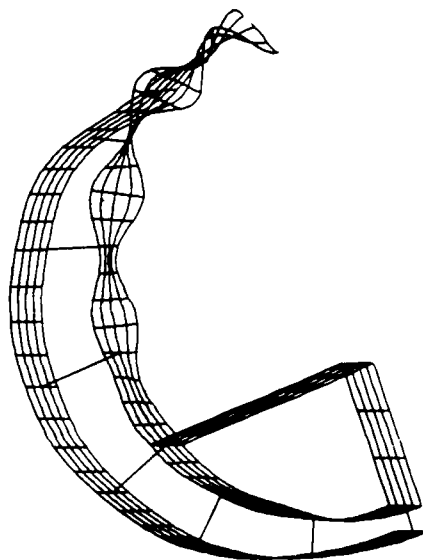


Figure 39: Minimum Interframe Buckling Mode Shape for Complete Submarine Section - Model 10

The longitudinal mode shape for all of the interframe models was a half sine wave centered at the stiffener. This is equivalent to a half sine wave shape between stiffeners as expected.

5.2.4 Plastic Collapse Results

Line four of Table 2 gives the plastic collapse loads of the various models including secondary structure obtained using ADINA. The dent and cutout models collapsed at loads lower than the pressure hull alone. The higher stresses induced by these features caused collapse mechanisms to form in the cutout and dent regions before the remainder of the pressure hull reached yield.

The deck-trim tank and ballast tank models showed no change in the collapse load over the axisymmetric pressure hull alone. Localized stress increases occurred but did not result in the formation of hinge mechanisms before the shell interframe collapse mechanism formed.

No value is given in the table for the full structure as ADINA was unable to accept part of the modelling for this case. It is expected that the cutout would produce a lower collapse load for this case.

The attainment of yield collapse of the axisymmetric pressure hull was primarily linear

behaviour. There was no occurrence of geometric nonlinearity via large displacements until the point of failure. Some ductility in the material after reaching yield occurred through strain hardening; however, collapse occurred at a pressure only marginally greater than the pressure to cause initial yielding determined by linear analysis. The geometry of the pressure hull appears to be such that linear predictions of the collapse pressure would be quite accurate. The dent model indicated more ductility before collapse as did the cutout model and a nonlinear analysis may be warranted for these cases.

5.3 Strain Measurements

Results of stress derived from strain measurements on an Oberon class hull at the three locations are shown in Table 3 and compared with finite element predictions. The locations are given in Figure 21 and the direction of stress is indicated in the table by the letter a, for axial, and the letter c, for circumferential directions.

Location	Direction	Experiment	Finite Elem	% Difference
A 70°	Midbay c	0.92	1.0	7.8
B 60°	Midbay c	0.87	1.0	12.7
	Stiffener c	0.94	1.01	7.3
	Stiffener a	0.56	0.49	14.6
C 30°	Midbay c	0.84	1.01	17.1

Table 3: Comparison - Experimental and Theoretical Nondimensional Stress Values

There are several possible causes of the difference between the experimental and analytical results. The most prevalent cause is the finite element modelling. In order to give the correct boundary conditions in the finite element model, the entire forward end of the submarine from the watertight bulkhead to the dome endcap was modelled. This resulted in a fairly coarse element grid. There was also no secondary structure modelled in addition to the pressure hull. Considerable secondary structure is present in this region (deck, tanks, fairing, ballast tank, cutout reinforcements) and would make the pressure hull stiffer and result in lower stress values than were predicted. Other nonstructural material such as cableways, piping, insulation, etc. would also add marginally to the pressure hull stiffness.

The distribution of weight, primarily fluids, on the submarine was not recorded during the trials and the redistribution that occurs during operation would have some effect on the stress values in the hull. This is supported by the fact that the strain gauge readings did not return

to zero upon resurfacing and were different by as much as 30 microstrains in the circumferential direction which translates to a stress of 6.2 MPa. This would have the effect of making the experimental stress measurements smaller than they may have actually been.

Inaccuracies in the depth of the submarine which was read from a pressure gauge could also result in differences between the analytical and experimental values. A depth variation of 1 metre would alter the circumferential stress by approximately 1 MPa.

6 Conclusions

The four methods used to study the structural characteristics of the axisymmetric pressure hull alone compared reasonably well. The Bryant equation was somewhat unconservative for the overall buckling load as a result of not including interstiffener shear deformation, although still quite acceptable for design approximations. The classical equations are the simplest to use but they do not give the flexibility that may be required for a structure with different boundary conditions, nonuniform axisymmetric stiffening or loading or non-axisymmetric structural components.

Including non-axisymmetric structure produced buckling loads, mode shapes and stress patterns which differed significantly from the axisymmetric structure results. As expected, dents and cutouts in the pressure hull lowered the overall buckling loads, increased local stresses and changed the buckling mode shapes considerably. The deck and trim tank stiffened the structure and raised both the overall and interframe buckling loads and also raised stresses in the region of the deck-hull intersection. The external ballast tank increased the overall buckling load of the pressure hull moderately. The interframe buckling load was increased considerably by the deck-trim tank and external ballast tank.

An analysis of the complete submarine section indicated buckling loads greater than or equal to those predicted considering the axisymmetric pressure hull alone. This gives confidence to the use of simplified methods for determining bifurcation buckling loads. Generally, deck and tank structure are located throughout most of the pressure hull and appear to serve as an added safety margin in buckling predictions. Careful attention should be paid to detailing of cutouts to avoid large stress concentrations. The influence of large openings on the overall behaviour of the pressure hull should be studied by three dimensional finite element methods where possible. The values obtained for collapse, interstiffener bifurcation buckling and overall bifurcation buckling agreed closely with the design safety factors of 1.5, 2.5 and 3.5 respectively.

There was reasonable agreement between the experimental and analytical stress values from the Oberon pressure hull. It is interesting to note that there is a decrease in the experimental stress values as the circumference is traversed from near the deck to the top of the pressure hull. This supports the stress results of the full three dimensional finite element models which showed this same trend.

Some of the results of this study have led to further questions requiring extensive study on their own. Because plastic collapse is the ultimate failure mode of the submarine, a detailed study including plastic hinge formation, local yielding and instability of the stiffeners, stress concentrations, out of roundness and residual stress should be undertaken to better establish the failure mechanism. The effects of damage such as dents on the structural response of the pressure hull is a subject of current research and is in need of a considerable amount of study.

Finally, this study also served as a mechanism to demonstrate the use of the various software packages at DREA for submarine structural analysis. The collection of programs used for model

generation, analysis and result interpretation proved to be a comprehensive and useable package for this study.

7 References

1. British Standard Specification for Unfired Fusion Welded Pressure Vessels, British Standard Institution BS5500, Issue 5, April 1980.
2. Gill S.S., 'The Stress Analysis of Pressure Vessels and Pressure Vessel Components', Pergamon Press, 1970.
3. Salerno V.L., Pulos J.G., 'Stress Distribution in A Circular Cylindrical Shell Under Hydrostatic Pressure Supported by Equally Spaced Circular Ring Frames', Polytechnic Institute of Brooklyn Report No. 171-A, June 1951.
4. Lunchick M.E., 'Yield Failure of Stiffened Cylinders Under Hydrostatic Pressure', David Taylor Model Basin Report 1291, January 1959.
5. Pegg N.G., Smith D.R., 'PRHDEF - Stress and Stability Analysis of Ring Stiffened Submarine Pressure Hulls', Defence Research Establishment Atlantic Technical Memorandum 87/213, Dartmouth, Canada, 1987.
6. SUBHUL User's Guide, NUCON Engineering and Contracting, Rotterdam, September, 1986.
7. Bushnell D., 'BOSOR4: Program for Stress, Buckling and Vibration of Complex Shells of Revolution', Structural Mechanics Laboratory, Lockheed Missiles and Space Co. Inc., Palo Alto, California.
8. Bushnell D., 'BOSOR5: A Computer Program for Buckling of Elastic-Plastic Complex Shells of Revolution Including Large Deflections and Creep', User's Manual, Lockheed Missiles and Space Co. Inc., Sunnyvale, California, 1974.
9. 'Vibration and Strength Analysis Program (VAST), Version 04', Martec Ltd, Halifax, Nova Scotia, DREA Contract Report CR 86/429, Dartmouth, N.S., 1986.
10. 'ADINA, A Finite Element Program for Automatic Dynamic Incremental Nonlinear Analysis', User's Manual, ADINA Engineering Inc., Watertown, Mass., September 1981.
11. Robertson K.A., 'Finite Element Analysis of a Short Submarine Compartment with Decks', MSc Project, University College London, October 1984.

Unclassified

SECURITY CLASSIFICATION OF FORM
Highest classification of Title, Abstract, Keywords

DOCUMENT CONTROL DATA

(Security classification of title, body of abstract and enclosing annotation must be entered when the overall document is classified)

1. ORIGINATOR (the name and address of the organization preparing the document. Organizations for whom the document was prepared, e.g. Establishment sponsoring a contractor's report, or tasking agency, are entered in section 8)		2. SECURITY CLASSIFICATION (Overall security classification of the document including special warning terms if applicable)	
Defence Research Establishment Atlantic		Unclassified	
3. TITLE (the complete document title as indicated on the title page. Its classification should be indicated by the appropriate abbreviation (S.E.R or U in parentheses after the title)) Effects of Secondary Structure on the Stress and Stability of Axisymmetric Submarine Pressure Hulls			
4. AUTHORS (last name, first name, middle initial if military, show rank, e.g. Gen. Maj. John E.) Pegg, N.G.			
5. DATE OF PUBLICATION (month and year of publication of document) NOVEMBER 1987	6a. NO. OF PAGES (total containing information, include Annexes, Appendices, etc.) 45	6b. NO. OF REFS (total cited in document) 11	
7. DESCRIPTIVE NOTES (the category of the document, e.g. technical report, technical note or memorandum. If appropriate, enter the type of report, e.g. interim, progress, summary, annual or final. Give the inclusive dates when a specific reporting period is covered.) DREA Report			
8. SPONSORING ACTIVITY (the name of the department, project office or laboratory sponsoring the research and development, include the address) Defence Research Establishment Atlantic			
9a. PROJECT OR GRANT NO. (if appropriate, the applicable research and development project or grant number under which the document was written. Please specify whether project or grant)	9b. CONTRACT NO. (if appropriate, the applicable number under which the document was written)		
10a. ORIGINATOR'S DOCUMENT NUMBER (the official document number by which the document is identified by the originating activity. This number must be unique to this document) DREA REPORT 87/102	10b. OTHER DOCUMENT NOS. (any other numbers which may be assigned this document either by the originator or by the sponsor)		
11. DOCUMENT AVAILABILITY (any limitations on further dissemination of the document, other than those imposed by security classification) <input checked="" type="checkbox"/> UNLIMITED DISTRIBUTION <input type="checkbox"/> Distribution limited to defence departments and defence contractors; further distribution only as approved <input type="checkbox"/> Distribution limited to defence departments and Canadian defence contractors; further distribution only as approved <input type="checkbox"/> Distribution limited to government departments and agencies; further distribution only as approved <input type="checkbox"/> Distribution limited to defence departments; further distribution only as approved <input type="checkbox"/> Other (please specify)			
12. DOCUMENT ANNOUNCEMENT (any limitation to the bibliographic announcement of this document. This will normally correspond to the Document Availability (11). However, where further distribution beyond the audience specified in 11 is possible, a wider announcement audience may be selected) Unlimited			

Unclassified

SECURITY CLASSIFICATION OF FORM

DDOCS: 9-04/87

Unclassified

SECURITY CLASSIFICATION OF FORM

13 ABSTRACT (a brief and factual summary of the document. It may also appear elsewhere in the body of the document itself. It is highly desirable that the abstract of classified documents be unclassified. Each paragraph of the abstract shall begin with an indication of the security classification of the information in the paragraph (unless the document itself is unclassified) represented as (S), (C), (U), or (E). It is not necessary to include here abstracts in both official languages unless the text is bilingual).

This report presents an investigation into the localized effects of secondary structure such as decks, tanks and cutouts, and other deviations from axisymmetry on the global failure load estimation of axisymmetric submarine pressure hulls. Three dimensional finite element analysis predictions of stress, elastic bifurcation buckling and nonlinear collapse loads of a representative complete section of a conventional submarine are compared to those of axisymmetric analysis methods applied to the pressure hull alone. Four different methods of analyzing the basic axisymmetric pressure hull are also compared. Stress patterns, buckling mode shapes and failure loads of the fully developed structural models were found to differ significantly from those obtained assuming complete axisymmetry. The inclusion of decks and tanks increased the failure loads, whereas cutouts and dents in the pressure hull lowered the failure loads. In addition to analytical results, experimental stress measurements made on an Oberon class pressure hull are compared to finite element predictions.

14 KEYWORDS, DESCRIPTORS or IDENTIFIERS (technically meaningful terms or short phrases that characterize a document and could be helpful in cataloguing the document. They should be selected so that no security classification is required. Identifiers, such as equipment model designation, trade name, military project code name, geographic location may also be included, if possible. Keywords should be selected from a published thesaurus, e.g. Thesaurus of Engineering and Scientific Terms (TEST) and their thesaurus identified. If it is not possible to select meaning terms which are Unclassified, the classification of each should be indicated as with the term.)

Submarine structures
Finite elements
Buckling
Stress
BOSOR
ADINA
Linear structural analysis
Nonlinear structural analysis
Ring stiffened cylinders

Unclassified

SECURITY CLASSIFICATION OF FORM

END

DATE

FILMED

6-88

DTIC